COMMUNICATION

"Chemical Blowing" of Thin-Walled Bubbles: High-Throughput Fabrication of Large-Area, Few-Layered BN and C_x-BN Nanosheets

Xuebin Wang, Chunyi Zhi,* Liang Li, Haibo Zeng, Chun Li, Masanori Mitome, Dmitri Golberg,* and Yoshio Bando*

Two-dimensional (2D) crystals have displayed unique potentials in energy, catalysis, superconductivity, and electronics fields because of their low dimensions and special edge structures.[1,2] Among the 2D crystals, sp^2-hybridized graphene and its sister, monolayered hexagonal boron nitride (*h*-BN, so-called "white graphene"), may be equally attractive for fundamental physics and diverse functionalities. BN atomic sheets conventionally show excellent deep UV luminescence[3,4] and superb lubrication.[5] Their composites with polymers or bioceramics exhibit extraordinary thermoconductive and mechanical properties.[6,7] They can also serve as a dielectric gate layer,[8] as well as an edge-tailored bandgap-tunable semiconductor,[9] and as a substrate able to enhance the carrier mobility[10] and to open the bandgap in graphene.[11,12] They are the perfect "sidekick" of graphene in next-generation electronics. Moreover, merging "black" (i.e., carbon) and "white" (i.e., BN) graphenes, B–C–N atomic sheets may be envisioned as an important congener for flat electronics, providing a smart approach to semiconductivity.[13] In fact, the potentially tunable bandgaps of the B–C–N system will enable its outstanding functional flexibility in luminescence and electronics.[14]

Graphene chemical exfoliation can yield a sufficient mass of a product. By contrast, although the methods of mechanical cleavage,[15,16] solution exfoliation,[6,7,17] high-energy electron beam irradiation,[18] reaction of boric acid and urea,[19,20] unwrapping nanotubes,[9] and chemical vapor deposition (CVD)[14,21–24] have already been reported for the preparation of BN and B–C–N atomic sheets, it is noted that it is still a challenge to reliably chemically delaminate and/or exfoliate BN and B–C–N layers and to realize mass production of atomically thin sheets made of those materials. The stronger interlayer coupling in BN compared with graphite should account for the unfavorable situation. The lack of mass production for BN and B–C–N atomic sheets causes a delay in their studies and technological tests in composites and electronic devices, in sharp contrast with graphene. Here, we report on a new approach, "chemical blowing", which relies on making large bubbles with atomically thin B–N–H (or B–N–C–H) polymer walls by releasing hydrogen gas (H_2) from a precursor ammonia borane (AB) compound, somewhat resembling blowing up a balloon. Numerous mono- and few-layered BN or C_x–BN sheets with large lateral dimensions are produced with an exceptionally high throughput after high-temperature annealing and collapse of the polymer bubbles. Using the prepared nanosheets, two of the many potential practical impacts are demonstrated, namely, mechanical reinforcement of a polymer using BN nanosheets and tunable conductivities in semiconducting C_x–BN nanosheets. This would provide a new method for the synthesis of 2D crystals and enable the potential applications of BN and C_x–BN nanosheets.

The as-grown BN nanosheets are often larger than 100 μm in lateral dimension and uniform over the whole area, as revealed by optical and scanning electron microscopy (SEM) images (**Figure 1**a,b). Their typical thickness is measured to be ≈2 nm by atomic force microscopy (AFM, Figure 1c) and generally ranges from 1 to 5 nm, although a few sheets thicker than 10 nm have also been found. High-resolution transmission electron microscopy (HRTEM) observations reveal the sheets with a different number of layers, from 1 to 7, as depicted in Figure 1d–f and Supporting Information Figure S3. A layer-to-layer distance is 0.35 nm, slightly larger than that in bulk layered BN due to surface atom relaxation. Overall, the production yield of BN sheets is as high as 25 wt%, related to the starting raw AB weight, thus significantly higher than those in methods of CVD and solution exfoliation.[6] The achieved yield and lateral dimensions of nanosheets are large enough for further assembly of nanoelectronic devices and fabricating nanosheet-containing composites.

The polycrystalline structure of a double-layer BN sheet is further verified by HRTEM together with a selected area electron diffraction (SAED) pattern (**Figure 2**a,b). The distance between the two neighboring bright reflections in the inset of Figure 2a perfectly corresponds to the B–B or N–N atom separations in *h*-BN, as also further confirmed by an X-ray diffraction (XRD) profile (Figure 2c). The (002) peak with a *d* value of 0.35 nm matches well with that derived from the HRTEM data. Its broadening corresponds to the effect of downsized dimensions with a size of 2.9 nm calculated from the Scherrer formula.[25] Such value is close to the determined nanosheet thickness.

Dr. X. B. Wang, Dr. C. Y. Zhi, Dr. L. Li, Dr. H. B. Zeng, Dr. C. Li, Dr. M. Mitome, Prof. D. Golberg, Prof. Y. Bando
International Center for Materials Nanoarchitectonics (MANA)
National Institute for Materials Science (NIMS)
Namiki 1-1, Tsukuba, Ibaraki 305-0044, Japan
E-mail: Wangxb@fuji.waseda.jp; ZHI.Chunyi@nims.go.jp; GOLBERG.Dmitri@nims.go.jp
Dr. X. B. Wang, Prof. Y. Bando
Department of Nano-Science and Nano-Engineering
Faculty of Science and Engineering
Waseda University
Okubo 3-4-1, Shinjuku-ku, Tokyo 169-8555, Japan

DOI: 10.1002/adma.201101788

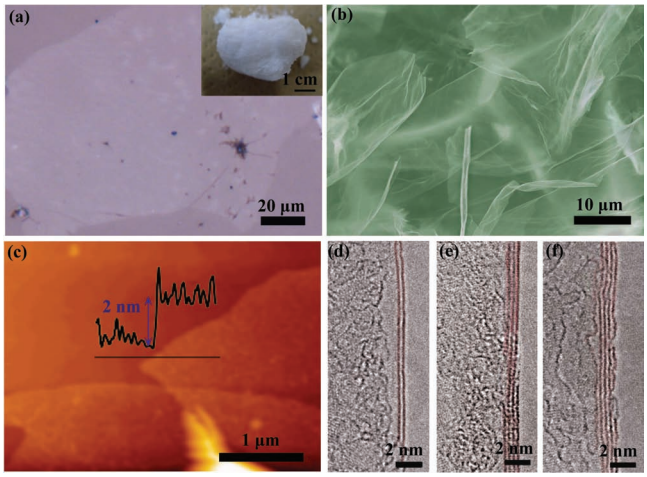

Figure 1. Morphology of BN nanosheets. a) Optical image of a large BN nanosheet transferred on a SiO_2 substrate. The inset shows a "snow-white" BN specimen. b) SEM image of ultrathin BN sheets. c) AFM image of BN sheets on a SiO_2 substrate pointing at their thickness of ≈2 nm. The inset shows the corresponding cross-sectional profile. d–f) HRTEM images of BN nanosheets with two, three, and four-to-five atomic layers.

As-synthesized C_x–BN atomic sheets with different C contents were analyzed by electron energy-loss spectroscopy (EELS, Figure 2d). The C contents were 14, 18 and 27 at% for the three representative nanosheets, denoted as $C_{0.3}$-BN, $C_{0.4}$-BN, and $C_{0.7}$-BN, respectively. The *K*-edge absorptions of B, C, and N atoms exhibit the sharp peaks followed by wider bands corresponding to the 1s–π* and 1s–σ* transitions, respectively. This is a clear characteristic of the sp^2-hybridization, indicating the hexagonal arrangement of B, C, and N atoms in the sheets. There are no obvious changes in the morphology between C_x–BN and BN nanosheets, but the material's color changed: the C_x–BN product appears grayer or darker compared to the snow-white BN product (Supporting Information Figure S4). In agreement with the color changes, the light absorption in the visible range increases with increasing C content (Figure 2e). The absorption spectra of C_x–BN nanosheets show two separated bands: the absorption peak at 210 nm with an absorption edge of 5.4 eV is attributed to *h*-BN, while the wide absorption band stretched from 200 to 800 nm with an absorption edge of 0.4 eV is similar to graphene's absorption and caused by C additives (see details in Supporting Information Figure S5). This implies the existence of a phase-separated structure made of BN and C domains. Phase-separated C_x–BN has much fewer C–N and C–B bonds than a homogeneous B–C–N, which is verified by the X-ray photoelectron spectroscopy (XPS) analysis (Supporting Information Figure S6). Further, we identified many ≈10 nm C islands that may be regarded as graphene quantum dots attached on the surface of BN matrices during detailed spatially resolved EELS mappings. First-principles calculations indicate that small gaps are opened mainly because of quantum confinement in these superlattice-like C networks,[26,27] qualitatively explaining the nonzero optical

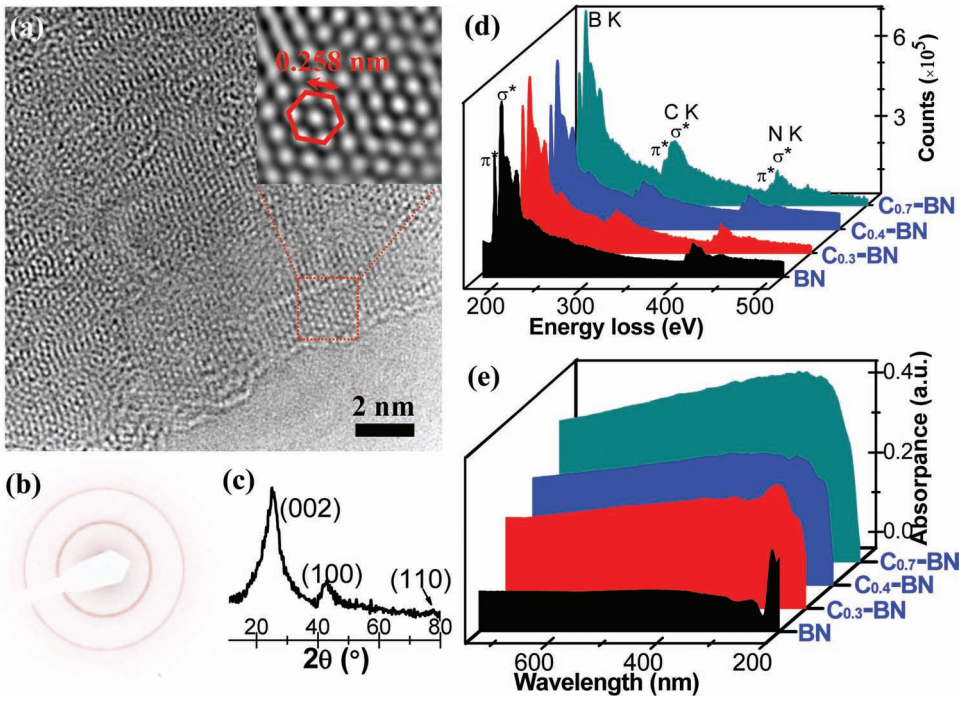

Figure 2. Structure and composition of BN and C_x–BN nanosheets. a) HRTEM image of a BN sheet revealing a polycrystalline structure. The inset is reconstructed reverse fast Fourier transform image from the framed area. b) SAED image of a BN nanosheet with continuous diffraction rings implying the existence of a polycrystal. The image was taken with an aperture covering 100 × 100 nm^2. c) XRD profile of BN sheets confirming a hexagonal structure of the space group 194 (JCPDS card No. 34-0421). d) EEL spectra of C_x–BN nanosheets manifesting a different C content. e) UV-vis diffuse reflection spectra of C_x–BN sheets highlighting their absorption and optical bandgaps.

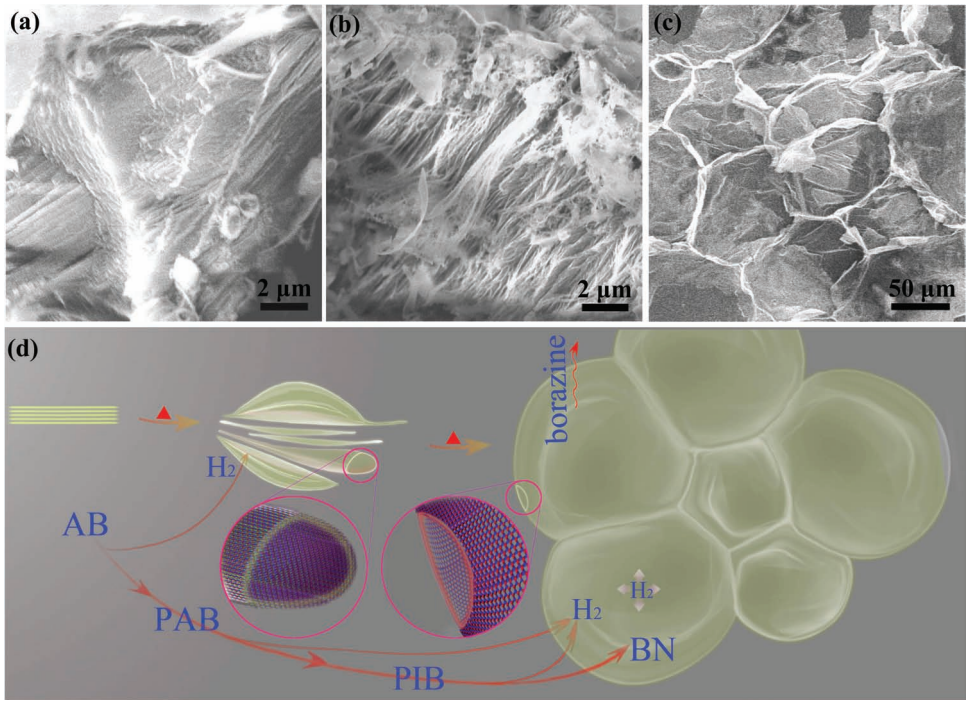

Figure 3. Growth process of BN nanosheets under proposed chemical blowing. a) SEM image of a raw AB molecular crystal with the ribbon-like morphology at room temperature. b) Morphology of the slightly disordered ribbon-stack of an intermediate obtained after pretreatment at 80 °C for 30 min. c) Morphology of an intermediate (produced at 400 °C) showing densely packed bubbles connecting with each other in a manner resembling a soap foam. d) A sketch explaining the growth process during the chemical blowing that consists of self-bubbling of a B–N–H polymer under dehydrogenation until it has atomically thin walls.

absorption edge (see details in Supporting Information Figure S8–10).

The fabrication process of nanosheets is further documented in **Figure 3** and Supporting Information Figure S11. During pyrolysis of AB, a ribbon-like matter becomes slightly fuzzy and disordered with an increase in reaction activity after pretreatment at 80 °C, probably because of conversion to a new mobile phase.[28] Subsequently, the new-phase AB is dehydrogenated and fully translates into polymeric aminoborane (PAB) at 120 °C, then to polyiminoborane (PIB) at 160 °C, then to BNH_δ at 400 °C, and finally to BN at 1200 °C, demonstrating a similar chemical change as reported previously.[29] Since it is noticed that BNH_δ is made of densely packed bubbles, we propose an original growth mechanism named by us as "chemical blowing" herein. First, an activated new-phase AB starts to change into PAB around 100 °C, starting a H_2 release that initiates the blowing of soft PAB polymers into bubbles. The polarity of B–N bonds may contribute to the formation of plane-like structures of polymers that can effectively trap the released gas. Then, due to self-heating, the transformation from AB via PAB to PIB is quickly completed. Quickly released H_2 effectively blows bubbles until their walls become very thin. Along with this process, some small molecules, such as borazine, are also lost,[30] which further intensifies the thinning process. Finally, polymeric walls of bubbles change into solid BN at a high temperature accompanied with dehydrogenation and then convert into atomically thin sheets after bubble crushing and/or collapse. For C_x–BN sheets, ethanol is introduced after the temperature reaches 500 °C to cause graphitization. At this temperature the structure of BNH_δ with a small amount of H is stable enough to prevent the formation of nanosized C domains within the BNH_δ walls. Hence, C domains mainly attach to the BN matrices' surfaces, as stated above.

The abundant production of BN atomic sheets enables us to perform a follow-up study of their performance in composites. We fabricated a novel polycarbonate (PC, which is typically used as an engineering plastic)/BN nanosheet composite. The composite film, with a thickness around 20 μm, retains high transparency with transmission of 70% in the whole visible range (**Figure 4**a). The elastic modulus and yield strength of PC/BN composites were dramatically enhanced by dozens of percents as a result of BN nanosheet embedment (Figure 4b). The reinforcement probably results from an effective transfer of a mechanical load to the BN nanosheets, which provide large-area long interfaces with PC and enhance the interfacial interactions per unit mass of an additive due to their ultrathin thicknesses.

C_x–BN nanosheets (100-μm) with surface-attached, few-layered C domains provide wide enough areas to be utilized in many electronic devices with unique electrical characteristics. In fact, the precisely tuned conductivity has been demonstrated in this work (Figure 4c). Pure BN nanosheets are electrical insulators, whereas C_x–BN sheets become semiconductors with a controlled resistivity varying in a large range, from 10^2 to 10^{-1} Ω m, depending on the C content. Somewhat weaker conductivity of C_x–BN nanosheets compared with graphene results from the

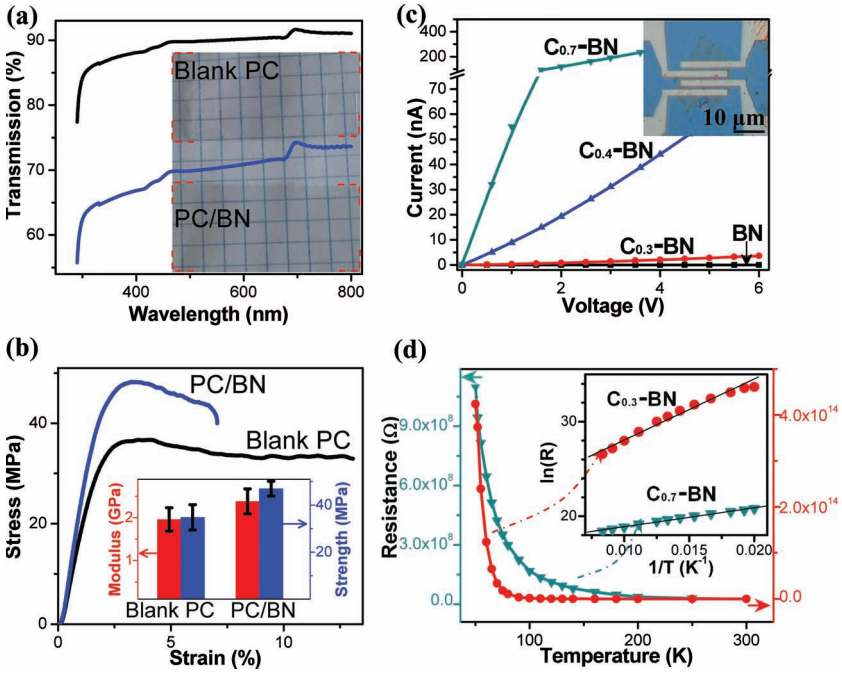

Figure 4. Mechanical performance of PC/BN composites and electrical properties of C_x–BN nanosheets. a) High optical transparency is preserved in PC/BN composites. The inset shows PC and PC/BN films. b) Stress–strain curves showing enhanced tensile strength of PC/BN composites. The inset shows the elastic modulus and yield strength increases by 22% and 35%, respectively, for PC/BN with a 2 wt% BN loading fraction. c) Current–voltage characteristics of BN and C_x–BN nanosheets measured at room temperature with the same geometry of a conducting channel. The used four-electrode device is shown in the inset; the two neighboring electrodes serve as a drain and a source. d) Temperature (T)-dependent resistance (R) of C_x–BN nanosheets. The inset shows linear fitting of ln(R) function over T^{-1} in a 50–200 K range.

existence of spatial gaps between the C domains. The resistivity of C_x–BN nanosheets rapidly increases under cooling, reflecting a typical semiconductor behavior (Figure 4d), well described by $R \propto e^{E/k_B T}$ where E is the bandgap and k_B is Boltzmann's constant.[14] The thermal bandgaps are calculated as 56 and 17 meV for $C_{0.3}$–BN and $C_{0.7}$–BN compositions qualitatively consistent with the bandgaps' values derived from the first-principles calculations. Tunable bandgaps of the hybridized heterogeneous C_x–BN structures behave similarly to those of graphene nanohole superlattices.[31]

In summary, we have developed a new route of chemical blowing for the production of atomically thin (one-to-few atomic layers) free-standing BN and C_x–BN nanosheets. This technology has two main characteristic features: high volume yield and laterally large areas. These not only provide large enough flakes that are readily available for electrical and mechanical performance explorations, but also give enough nanosheet mass for fabricating ultimately strong polymeric or other composites. Significant mechanical reinforcement in PC/BN composites and delicate tuning of nanosheet conductivity through modifying C contents in them are demonstrated in this work. Additionally, this catalyst- and substrate-free method is simpler than a normal CVD method and its products generally possess larger lateral dimensions than those obtained during solution-exfoliation methods. The developed technique opens up a wide horizon for the analogous growth of other 2D nanosheets and full realization of their potentials in nanotechnology.

Experimental Section

Synthesis: The detailed synthetic procedures for BN and C_x–BN sheets is shown in the Supporting Information, Figure S1. Briefly, the commercial fresh AB (Aldrich) was heated through a multistage process to produce BN bubbles, which then collapsed and converted into BN sheets. If ethanol was introduced in the above process, the C_x–BN sheets were obtained.

Characterization and Application: The as-grown product was dispersed in ethanol by ultrasonic treatment for 30 s. Then the suspension was transferred onto desired substrates for characterization and making devices. The morphology and structure were analyzed by SEM (Hitachi S-4800), HRTEM (JEOL JEM-3100FEF with Omega Filter), AFM (JEOL JSPM-5200), XRD (Rigaku Ultima III), UV-Vis (Jasco V-570) and IR (Thermo Nicolet 4700 FT-IR). The chemical state and composition were characterized by X-ray photoelectron spectroscopy (XPS) (Thermo Scientific Escalab 250Xi) and thermogravimetry/differential scanning calorimetry (TG/DSC) (Rigaku Thermo plus TG 8120/EVO DSC8230). Tensile tests were carried out using an EZ-S-100N machine (Shimadzu Co.). The patterns on electronic devices were drawn by electron beam lithography (Elionix, ELS-7500EX), and the electrodes of Ti/Au (10 nm/100 nm) were deposited using an electron beam evaporation system (ULVAC UEP-300-2C). Electrical measurements were performed with a Keithley 4200-SCS apparatus.

Supporting Information

Supporting Information is available from the Wiley Online Library or from the author.

Acknowledgements

The authors are grateful to Drs. Akihiko Nukui and Isamu Yamada for experimental support. The authors acknowledge support from JSPS Grant-in-Aid for Young Scientists. The authors are indebted to MANA of NIMS for financial support.

Received: May 12, 2011
Revised: June 20, 2011
Published online: August 2, 2011

[1] A. K. Geim, K. S. Novoselov, *Nat. Mater.* **2007**, *6*, 183.
[2] T. Greber, in *Handbook of Nanophysics*, (Ed: K. D. Sattler), CRC Press, Boca Raton, FL **2010**, Ch. 18.
[3] K. Watanabe, T. Taniguchi, T. Niiyama, K. Miya, M. Taniguchi, *Nat. Photonics* **2009**, *3*, 591.
[4] K. Watanabe, T. Taniguchi, H. Kanda, *Nat. Mater.* **2004**, *3*, 404.
[5] C. Lee, Q. Li, W. Kalb, X. Z. Liu, H. Berger, R. W. Carpick, J. Hone, *Science* **2010**, *328*, 76.
[6] C. Zhi, Y. Bando, C. Tang, H. Kuwahara, D. Golberg, *Adv. Mater.* **2009**, *21*, 2889.

[7] J. N. Coleman, M. Lotya, A. O'Neill, S. D. Bergin, P. J. King, U. Khan, K. Young, A. Gaucher, S. De, R. J. Smith, I. V. Shvets, S. K. Arora, G. Stanton, H. Y. Kim, K. Lee, G. T. Kim, G. S. Duesberg, T. Hallam, J. J. Boland, J. J. Wang, J. F. Donegan, J. C. Grunlan, G. Moriarty, A. Shmeliov, R. J. Nicholls, J. M. Perkins, E. M. Grieveson, K. Theuwissen, D. W. McComb, P. D. Nellist, V. Nicolosi, *Science* **2011**, *331*, 568.
[8] I. Meric, C. Dean, A. F. Young, J. Hone, P. Kim, K. Shepard, *IEDM Tech. Dig.* **2010**, *10*, 556.
[9] H. Zeng, C. Zhi, Z. Zhang, X. Wei, X. Wang, W. Guo, Y. Bando, D. Golberg, *Nano Lett.* **2010**, *10*, 5049.
[10] C. R. Dean, A. F. Young, I. Meric, C. Lee, L. Wang, S. Sorgenfrei, K. Watanabe, T. Taniguchi, P. Kim, K. L. Shepard, J. Hone, *Nat. Nanotechnol.* **2010**, *5*, 722.
[11] G. Giovannetti, P. A. Khomyakov, G. Brocks, P. J. Kelly, J. van den Brink, *Phys. Rev. B* **2007**, *76*, 073103.
[12] J. Slawinska, I. Zasado, Z. Klusek, *Phys. Rev. B* **2010**, *81*, 155433.
[13] T. B. Martins, R. H. Miwa, A. J. R. da Silva, A. Fazzio, *Phys. Rev. Lett.* **2007**, *98*, 196803.
[14] L. Ci, L. Song, C. Jin, D. Jariwala, D. Wu, Y. Li, S. A. Srivastava, Z. F. Wang, K. Storr, L. Balicas, F. Liu, P. M. Ajayan, *Nat. Mater.* **2010**, *9*, 430.
[15] K. S. Novoselov, D. Jiang, F. Schedin, T. J. Booth, V. V. Khotkevich, S. V. Morozov, A. K. Geim, *Proc. Natl. Acad. Sci. USA* **2005**, *102*, 10451.
[16] D. Pacile, J. C. Meyer, C. O. Girit, A. Zettl, *Appl. Phys. Lett.* **2008**, *92*, 133107.
[17] W. Q. Han, L. Wu, Y. Zhu, K. Watanabe, T. Taniguchi, *Appl. Phys. Lett.* **2008**, *93*, 223103.
[18] C. Jin, F. Lin, K. Suenaga, S. Iijima, *Phys. Rev. Lett.* **2009**, *102*, 195505.
[19] A. Nag, K. Raidongia, K. P. S. S. Hembram, R. Datta, U. V. Waghmare, C. N. R. Rao, *ACS Nano* **2010**, *4*, 1539.
[20] K. Raidongia, A. Nag, K. P. S. S. Hembram, U. V. Waghmare, R. Datta, C. N. R. Rao, *Chem. Eur. J.* **2010**, *16*, 149.
[21] A. Nagashima, N. Tejima, Y. Gamou, T. Kawai, C. Oshima, *Phys. Rev. Lett.* **1995**, *75*, 3918.
[22] M. Corso, W. Auwarter, M. Muntwiler, A. Tamai, T. Greber, J. Osterwalder, *Science* **2004**, *303*, 217.
[23] L. Song, L. Ci, H. Lu, P. B. Sorokin, C. Jin, J. Ni, A. G. Kvashnin, D. G. Kvashnin, J. Lou, B. I. Yakobson, P. M. Ajayan, *Nano Lett.* **2010**, *10*, 3209.
[24] Y. Shi, C. Hamsen, X. Jia, K. K. Kim, A. Reina, M. Hofmann, A. L. Hsu, K. Zhang, H. Li, Z. Y. Juang, M. S. Dresselhaus, L. J. Li, J. Kong, *Nano Lett.* **2010**, *10*, 4134.
[25] P. Scherrer, *Gottinger Nachr.* **1918**, *2*, 98.
[26] L. A. Ponomarenko, F. Schedin, M. I. Katsnelson, R. Yang, E. W. Hill, K. S. Novoselov, A. K. Geim, *Science* **2008**, *320*, 356.
[27] A. K. Singh, E. S. Penev, B. I. Yakobson, *ACS Nano* **2010**, *4*, 3510.
[28] A. C. Stowe, W. J. Shaw, J. C. Linehan, B. Schmid, T. Autrey, *Phys. Chem. Chem. Phys.* **2007**, *9*, 1831.
[29] S. Frueh, R. Kellett, C. Mallery, T. Molter, W. S. Willis, C. Kingondu, S. L. Suib, *Inorg. Chem.* **2011**, *50*, 783.
[30] T. B. Marder, *Angew. Chem. Int. Ed.* **2007**, *46*, 8116.
[31] W. Liu, Z. F. Wang, Q. W. Shi, J. Yang, F. Liu, *Phys. Rev. B* **2009**, *80*, 233405.